Journal of Computational and Applied Mechanics, Vol. 18, No. 1, (2023), pp. 85–95
DOI: 10.32973/jcam.2023.003

POST-EXTRAPOLATION FOR SPECIFIED TIME-STEP RESULTS WITHOUT INTERPOLATION, IN MOC-BASED 1D HYDRAULIC TRANSIENTS AND GAS RELEASE COMPUTATIONS

Abdallah A. Estuti
Department of Maintenance and Projects
National Oil Company – Tripoli Libya
P.O. Box 13665
aestuti@noc.ly
abdalla.estuti@gmail.com

E. Litvai†
Department of Fluid Mechanics
Budapest University of Technology and Economics,
H–1111 Budapest, Bertalan Lajos u. 4–6., Hungary

[Received: March 7, 2023; Accepted: May 18, 2023]

Abstract. The goal of the paper is to present a supplementary step called post-extrapolation. When applied to the well-known method of characteristics (MOC), this assures the continuous use of the specified time steps or regular numerical grid without interpolations during computations of transients in 1D 2-phase flow in straight elastic pipes. The new method consists of two steps, the first being a typical MOC step, where the C^- and C^+ characteristics start from regular nodal points, allowing for the point of intersection to differ from a regular one. After defining the variables there the method transforms it corresponding to the near regular grid point, using the first derivatives contained in the original, nonlinear, governing equations, as evaluated numerically from the variables got earlier in the neighboring nodes. The procedure needs no interpolations; it deals with grid-point values only. Instead of the Courant-type stability conditions, shock-wave catching and smoothing techniques help to assure numerical stability between broad limits of parameters like the closing time of a valve and the initial gas content of the fluid. Comparison by runs with traditional codes under itemized boundary conditions and measurements on a simple TPV (tank-pipe-valve) setup show acceptable scatter.

Keywords: MOC, gas release, post-extrapolation, shock catching, transients

1. Introduction

In this paper we would like to introduce a new method, or rather a supplementary step called post-extrapolation. It is applied to the well-known method of characteristic (MOC), which assures the continuous use of a regular grid $(\Delta x, \Delta t)$ defined by

$$\Delta x = a_0 \Delta t \tag{1}$$

where a_0 = constant, Δt = constant being a specific time step. Since grid point-values of the variables are used, no interpolations are necessary. This is in contrast to the traditional case, where the Courant-type numerical stability criteria need interpolation, especially in two-phase fluid where the changes in gas content cause steep variations in the pressure wave celerity a. These problems will be treated in the next sections. First the basic equations are introduced.

For 1D two-phase pipe-flow the momentum equation used reads:

$$\frac{\partial u}{\partial t} + u\frac{\partial u}{\partial x} = -\frac{1}{\rho}\frac{\partial p}{\partial x} - \frac{\lambda}{2D}u\,|u| - g\sin\alpha\,. \tag{2}$$

The density of the fluid ρ can be expressed by the void fraction V; by the density of the liquid ρ_w and by the density of the gas or air contained in the fluid ρ_g as

$$\rho = (1-V)\,\rho_w + V\rho_g\,. \tag{3}$$

This helps to introduce the dimensionless density ratio

$$R_o = \frac{\rho_w}{\rho} = \frac{1}{1-\left(1-\frac{\rho_g}{\rho_w}\right)V}\,. \tag{4}$$

With the pressure head defined by

$$P = \rho_w g H$$

and with volume flow rate $Q = uA$ the momentum equation can be transformed

$$\frac{\partial Q}{\partial t} + \frac{Q}{A}\frac{\partial Q}{\partial x} + R_o A g\frac{\partial H}{\partial x} + \frac{\lambda}{2DA}Q\,|Q| + gA\sin\alpha = 0. \tag{5}$$

The continuity equation

$$\frac{\partial \rho}{\partial t} + \frac{\partial}{\partial x}(\rho u) = 0 \tag{6}$$

can be transformed by introducing the celerity a of the pressure waves:

$$\frac{1}{a^2} = \frac{\partial \rho}{\partial p} \tag{7}$$

to

$$\frac{\partial p}{\partial t} + u\frac{\partial p}{\partial x} + a^2\rho\frac{\partial u}{\partial x} = 0\,, \tag{8}$$

$$R_o\frac{\partial H}{\partial t} + \frac{Q}{A}R_o\frac{\partial H}{\partial x} + \frac{a^2}{Ag}\frac{\partial Q}{\partial x} = 0\,. \tag{9}$$

2. Equations of characteristics

Since the first part of the new method requires the method of characteristics, the usual procedure (see e.g. Wylie & Streeter [1]) with governing equations (5) and (9) leads to the following equations for the characteristics $C^{\mp}$:

$$\frac{dQ}{dt} \mp Ro\frac{ga}{A}\frac{dH}{dt} + gA\sin\alpha + \frac{\lambda}{2DA}Q\,|Q| = 0\,, \tag{10}$$

$$\frac{dx}{dt} = \frac{Q}{A} \mp a, \tag{11}$$

where the negative sign refers to the C^- characteristic.

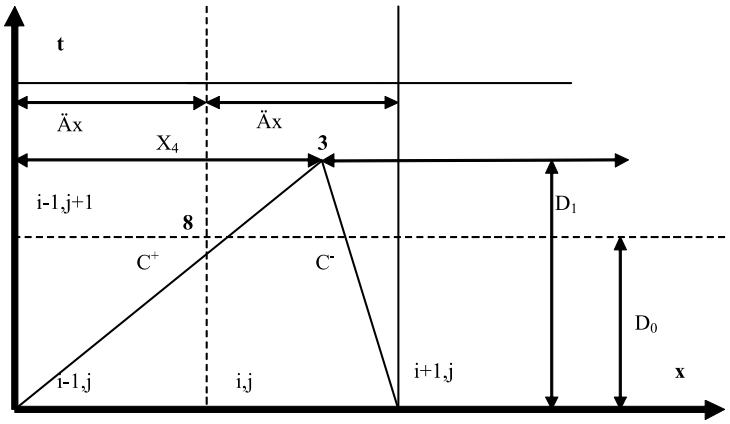

Figure 1. Notations of key nodal points in post-extrapolation

Figure 1 shows the point of intersection 3, the characteristic started in point $(i-1, j)$ and $(i+1, j)$, respectively. Its coordinates (x_4, D_1) can be taken from the equations for C^+

$$\left(\frac{dx}{dt}\right) = \frac{Q(i+1)}{A} + a(i) = \frac{x_4}{D_1}, \tag{12}$$

for C^-

$$\left(\frac{dx}{dt}\right) = \frac{U\,(i+1)}{A} - a(i) = \frac{x_4 - 2\Delta x}{D_1} \tag{13}$$

by introducing the following quantities

$$N_3 = \frac{Q\,(i-1) - U\,(i+1)}{A} + 2a(i)\,, \tag{14}$$

$$D_1 = 2\frac{\Delta x}{N_3}\,, \tag{15}$$

$$x_4 = D_1\frac{Q\,(i-1)}{A} + a(i)\,, \tag{16}$$

where $U\,(i+1) = Q\,(i+1)$ if $H\,(i+1) > H_v$, else see equations later. The values of the variables Q and H at point 3 in Figure 1, or U and H can be computed as usual by integrating equation (10) from t to $t + D_1$. From the integral along C^+ after transformations we obtain

$$H_3 = C_1 - B_1 Q_3 \tag{17}$$

with

$$C_1 = H\,(i+1) - BQ\,(i-1) - a\,(i)\,\frac{D_1}{R_o}\sin\alpha\,, \tag{18}$$

$$B_1 = B + R\,|Q(i-1)|\,\frac{a(i)}{\Delta x}D_1\,, \tag{19}$$

where

$$B = \frac{a(i)}{R_o g A}, \qquad R = \frac{\lambda\Delta x}{2gR_o D A^2}\,. \tag{20}$$

Similarly, integrating along C^- results in

$$H_3 = C_2 + B_2 Q_3 \,, \tag{21}$$

$$C_2 = H(i+1) - BQ(I+1) + a(i)\frac{D_1}{R_o}\sin\alpha \,, \tag{22}$$

$$B_2 = B + R\,|Q(i+1)|\,\frac{a(i)}{\Delta x}D_1 \,. \tag{23}$$

The difference of equations (17) and (21) yields

$$Q_3 = \frac{C_1 - C_2}{B_1 + B_2} \,. \tag{24}$$

It also holds that

$$H_3 = \frac{C_1 B_2 + C_2 B_1}{B_1 + B_2} \,. \tag{25}$$

Hence $U_3 = Q_3$.

If, however, $H_3 \le H_v$ then $H_3 = H_v$, i.e, cavity should be be prescribed. Then

$$U_3 = \frac{C_1 - H_v}{B_1} \qquad \text{instead of} \quad Q_3 \quad \text{and}$$

$$Q_3 = \frac{C_1 - H_v}{B_1} \,. \tag{26}$$

Their difference furnishes the rate of change of void fraction. Consequently,

$$V = \frac{(Q_3 - U_3)}{a_0 A} \,. \tag{27}$$

3. Post-extrapolation

The new element follows with the goal to transform the values of H_3, Q_3 or U_3 obtained in point 3 into values $H_8 = H(i, j+1)$, $Q_8 = Q(i, j+1)$ and $U_8 = U(i, j+1)$ in Figure 1. The transformation is based on the original nonlinear system of equations (5) and (9), defined by

$$K_h = H_8 - H_3 = (D_0 - D_1)\left[\frac{\partial H}{\partial t}\right]_3 + (\Delta x - x_4)\left[\frac{\partial H}{\partial x}\right]_3 , \tag{28}$$

$$K_q = Q_8 - Q_3 = (D_0 - D_1)\left[\frac{\partial Q}{\partial t}\right]_3 + (\Delta x - x_4)\left[\frac{\partial Q}{\partial x}\right]_3 . \tag{29}$$

The derivatives in brackets are expressed from the original equations (5) and (9) by the other partial derivatives, which in turn are computed as ratios of finite differences taken from the variables computed in the former steps in grid points $(i-1, j+1)$, $(i-1, j)$, (i, j) and $(i+1, j)$ in Figure 1. Consequently, equation (9) yields

$$\left[\frac{\partial H}{\partial t}\right]_3 = -\frac{a^2}{R_o g A}\frac{\Delta Q}{\Delta x} - \frac{Q}{A}\frac{\Delta H}{\Delta x} \,, \tag{30}$$

$$\left[\frac{\partial Q}{\partial t}\right]_3 = \frac{R_o g a}{a^2}\left(-\frac{\Delta H}{\Delta t} - \frac{Q}{A}\frac{\Delta H}{\Delta x}\right) . \tag{31}$$

In a similar manner equation (5) leads to the result

$$\left(\frac{\partial H}{\partial x}\right)_3 = \frac{1}{R_o g A}\left(-\frac{\Delta Q}{\Delta t} - \frac{\lambda}{2DA} Q\,|Q| - \frac{Q}{A}\frac{\Delta Q}{\Delta x} - gA\sin\alpha\right), \tag{32}$$

$$\left(\frac{\partial Q}{\partial t}\right)_3 = -R_o g A \frac{\Delta H}{\Delta x} - \frac{\lambda}{2DA} Q\,|Q| - \frac{Q}{A}\frac{\Delta Q}{\Delta x} - gA\sin\alpha\,. \tag{33}$$

The numerical derivatives are given by

$$\frac{\Delta H}{\Delta x} = \frac{(H\,(i+1,j) - H\,(i-1,j))}{2\Delta x}\,, \tag{34}$$

$$\frac{\Delta Q}{\Delta t} = \frac{(Q(i-1,j+1) - Q(i-1,j))}{D_0}\,. \tag{35}$$

After the derivatives in brackets have been defined K_h and K_q can be computed and the resulting variables

$$H_8 = H(i,j+1) = H_3 + K_h\,, \tag{36}$$

$$Q_8 = Q(i,j+1) = Q_3 + K_q \tag{37}$$

can be registered in the regular grid point $(i, j+1)$. As a last revision, only the condition $H_8 \le H_v$ remains. If true, then the restriction (even if approximated by) $H(i,j+1) = H_v$ must be made, since otherwise negative absolute pressure could appear.

The treatment of boundary conditions in the first (MOC) step is identical with the usual one. Since at the boundaries only one of the characteristics can be applied, point 3 lies on the boundary higher or lower than the grid point (or coincides with it). The derivatives in brackets with respect to x are thus equal to zero. The numerical derivatives are somewhat different.

4. Numerical stability

Because of the nonlinearity of the governing equations and of the after-extrapolation method, numerical instability and oscillation can appear during the computation, especially in the presence of cavities at vapor pressure or column separation caused by gas or air release. Experience during the programming stage of simulation of the TPV system showed that to attain numerical stability the application of a somewhat simplified version of Kranenburg's 'shock wave, nullifying cavitating flow region' model [2] and Vliegenthart's smoothing procedure [3] were necessary; they are compiled here. The jump through shock waves causes a decrease in the void fraction taken by the momentum equations in the form published by Kranenburg [2].

$$\frac{Q(i-1)}{A} + \frac{P(i-1) - P_v}{\rho_w a(i-1)} = B_1\,, \tag{38}$$

$$\frac{Q(i+1)}{A} + \frac{P(i-1) - P_v}{\rho_w a(i+1)} = B_2\,. \tag{39}$$

From the continuity

$$\Delta V = \frac{Q\,(i-1) - Q\,(i+1)}{A a_0}\,. \tag{40}$$

The pressure drop in the cavities caused by the gas released,

$$(P\,(i-1)-P_v)\,V\,A\,\Delta x = R_v T \Delta m \tag{41}$$

using the ideal gas law. The difference of momentum equations (38) and (39) yields the continuity in the form

$$a_0 \Delta V = B_1 - B_2 - \frac{P(i+1)-P_v}{\rho_w}\left(\frac{1}{a\,(i+1)}+\frac{1}{a\,(i-1)}\right). \tag{42}$$

The expressions B_1 and B_2 can be taken as

$$B_1 = \frac{Q\,(i-1)}{A} + g\frac{H(i-1)-H_v}{a(i)}\,, \tag{43}$$

$$B_2 = \frac{Q\,(i+1)}{A} + g\frac{H(i+1)-H_v}{a(i)} \tag{44}$$

according to the steps in MOC. Finally, mean values of H and a

$$\Delta V = \frac{Q(i-1)-Q(i+1)}{A a_0} - 2g\frac{H(i)-H_v}{a_0 a\,(i)} \tag{45}$$

are used as correction to the void fraction at the end of every time step if the condition $V > 0$ has been met. The corrected $V(i+1) = V(i) + \Delta V$ value is restricted to $V(i+1) \geq 0$.

The smoothing trick consisted of evaluating

$$L\,(i) = \frac{H(i+1)+H(i-1)}{2} - H(i)\,. \tag{46}$$

If $L(i) > 0$ then

$$H(i) = H(i) + \frac{L(i)}{2}, \qquad \text{else} \qquad L(i) = 0\,. \tag{47}$$

5. Accuracy

The accuracy of the new method has been judged by comparison in two steps. First it has been compared numerically with a traditional, "pre-interpolating" method, programmed and run under itemized boundary conditions and an identical numerical grid [4]. The arrangement computed is shown in Figure 2. It is prepared to measure and record the pressure history during and after closing the exit valve in three points of the TPV system. The asymptotic behavior of the system after closing the exit valve is followed numerically by computing the time history of:

1. the temporary maxima and minima of the fluctuating pressure at the exit valve, and
2. the time mean value of the fluctuating volume flow rate entering or leaving the pipe at the tank ($x = 0$), using both pre-interpolating and post-extrapolating methods.

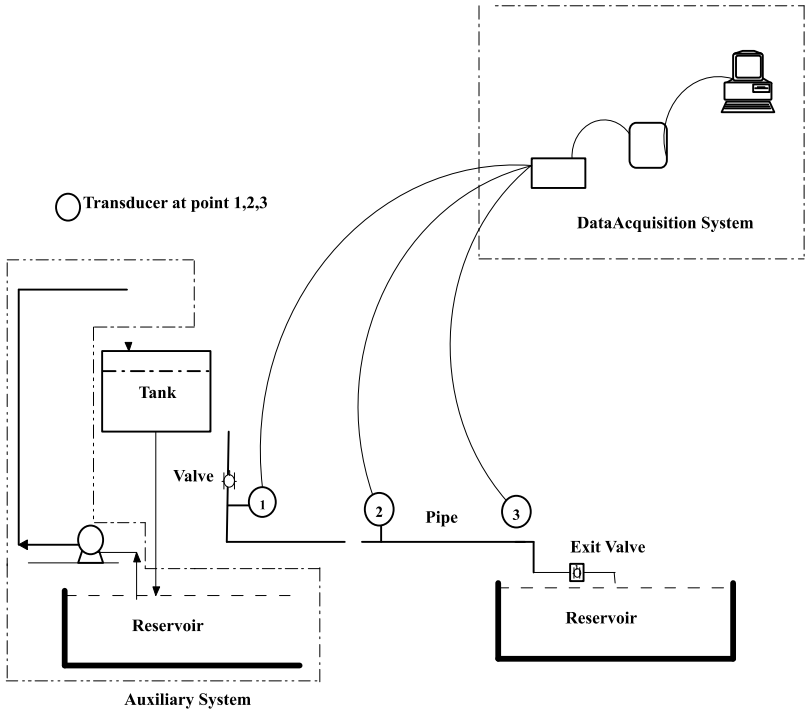

Figure 2. Experiment setup

The attenuation caused partly by the friction in the MOC method and partly by the additional artificial viscosity-like procedures in our method (which we call the New M method) appear in the asymptotic approximation of the limiting – static – value of the pressure as determined by the system data and by the zero flow rate. Some numerical runs with variable initial condition showed typical results after 104 time steps (nearly 30 times the duration of the closing time) of 0+3% or less of the limiting value as pressure fluctuation, and -10-5 as the ratio of the time mean flow rate to the initial flow rate; both values have been assumed as acceptable. Then as the second step the computed results have been compared with measured ones. Some results are shown in Figures 3 and 4 representing the middle and the endpoint, respectively. The agreement between the pre-interpolation (Simulation MOC) and post-extrapolation (Simulation New M) is remarkable. There are long time periods when the difference is less than 2% of the maximal pressure head measured. The deviations are greater near the second and third peak. They may be explained by the effect of the smoothing procedure, which should be improved, and possibly by the shock-wave capturing program, which could be refined: these two items are contained in the New M method and not in MOC. The measured pressure heads show somewhat greater deviation from both of the simulations above [5]. This can be explained partly by the usual errors in measuring

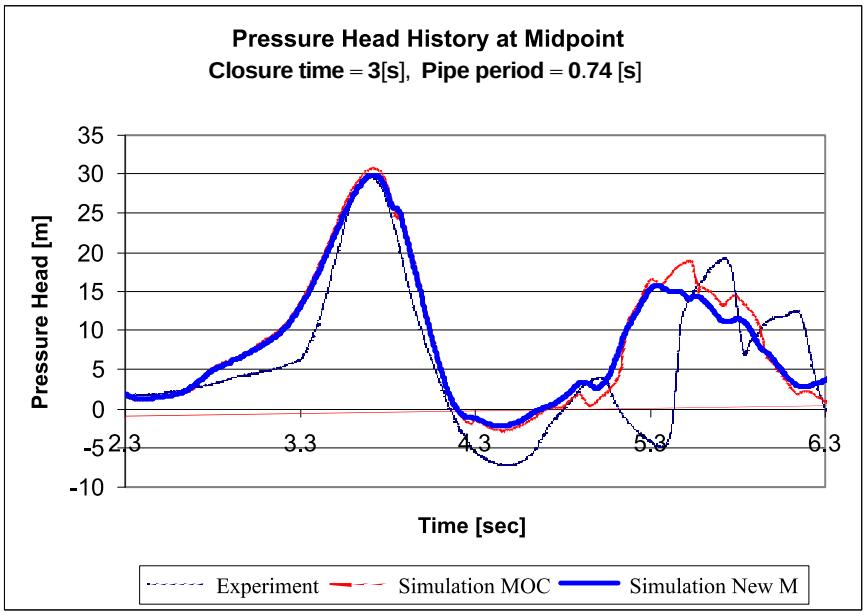

Figure 3. Pressure head history at midpoint of TPV system

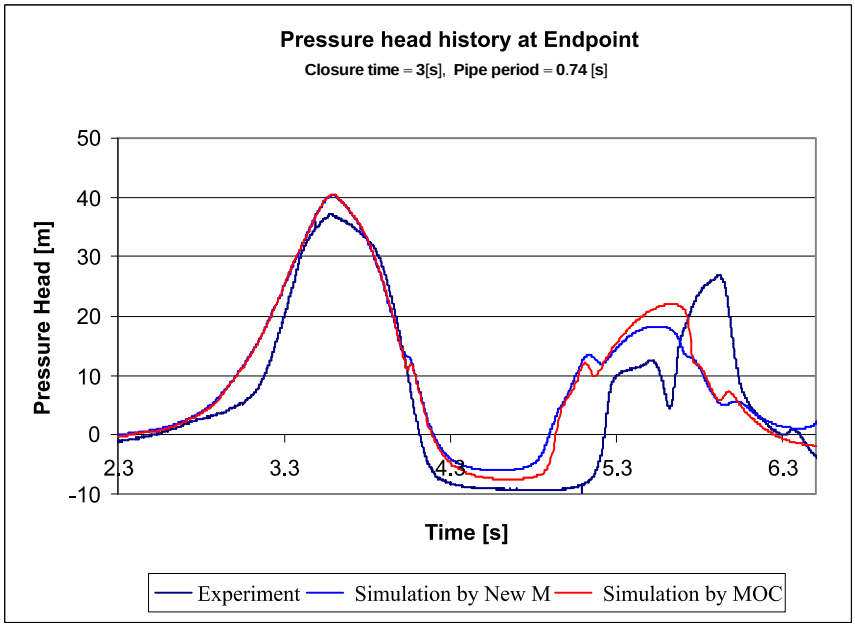

Figure 4. Pressure head history at endpoint of TPV system

equipment and methods (detailed in a special report [6]) and partly by the models of wave celerity and of gas release. It is very difficult to separate these factors without systematic modeling and measurements. Although a full description of the wave celerity and gas release models is beyond the scope of the present paper, we outline them below.

6. Celerity of pressure waves

The wave celerity a model used was based on results published by Wylie and Streeter [1] – see pp. 140–142 – after transformations in the form

$$\frac{a}{a_0} = \frac{H}{\sqrt{H^2 + mC_2}}\,, \tag{48}$$

where a_0 is the wave celerity in the fluid in the pipe without free gas or vapor,

$$C_2 = \frac{R_g T a_0^2}{\rho_w g^2}\,, \tag{49}$$

where m is the mass of free gas or vapor divided by the volume of the fluid.

The computed version is

$$m = m_1 = V\rho_v + m_3\,, \tag{50}$$

where m_3 $[kg/m^3]$ is the mass of the gas and/or air released and diffused in the cavities or contained in the incoming fluid in the unit of volume of fluid.

7. Cavity and gas release model

The incoming fluid is assumed to carry N_b homogeneously distributed cavitation nuclei in the unit of volume. Around the nuclei, there may be bubbles filled with gas (air) [7] and vapor, depending on the ambient pressure and temperature. The void fraction of the vapor is defined by equation (27) to be used in equation (50), on the condition that the pressure head is equal to the vapor pressure head H_v.

The mass of gas in unit volume of the fluid $m = m_3$ can be defined by

$$m = N_b \frac{D^3\pi}{6} \frac{\rho_w g H}{R_g T}\,, \tag{51}$$

or

$$\frac{m}{D^3 H} = N_b \frac{\pi}{6} \frac{\rho_w g}{R_g T} = S_n\,, \tag{52}$$

where D is the mean diameter of the bubbles and S_n is a known or guessed constant. The rate of the mass of gas released from the liquid and diffused into the bubbles has been calculated, following Kranenburg [2] by

$$\frac{\partial m}{\partial t} = N_b D^2 \pi \beta \frac{\partial c}{\partial r}\,, \tag{53}$$

where

$$\frac{\partial c}{\partial r} \cong \varepsilon \frac{c_0}{D\sqrt{\frac{\beta}{UD}}}\,. \tag{54}$$

With the initial concentration C_0 of the gas in liquid, according to Henry's law

$$C_0 = S_n \frac{\rho_w g H_{at}}{R_{air} T} \,. \tag{55}$$

Finally with $\varepsilon \approx 1$

$$\frac{\partial m}{\partial t} = F_c D^{\frac{3}{2}} \,, \tag{56}$$

$$F_c = N_b c_0 \pi \sqrt{\beta U} \,, \tag{57}$$

$$\frac{\partial m}{\partial t} \cong \frac{\Delta m_3}{D_0} \,, \tag{58}$$

$$\frac{D^3}{6} = V + \frac{m_3}{\rho_g} \,. \tag{59}$$

After each time step the diameter has been defined by equation (59), then Δm_3 from (58) and (56) then m_1 from equation (50) to continue with the new time step.

8. Conclusions

The introduction of the post-extrapolation, i.e. the use of the first partial derivatives of the governing equations, to define the variables after a MOC-type step at the regular grid points without pre-interpolation, proved to be successful in two-phase fluid flow with gas release and variable wave celerity in 1D elastic pipe transient flow computations. Instead of the Courant-type stability condition, simple shock-wave capturing and oscillation-smoothing techniques help to assure the numerical stability of the computations. The accuracy seems to correspond to traditional methods, although it can be influenced by the requirements of numerical stability [6, 7]. Measurements indicate the need for broader studies with respect to the appropriateness of the models of wave celerity and gas release used.

References

1. Wyle, E. B. and Streeter, V. L. *Fluid Transients in Systems.* McGraw-Hill, 1993.
2. Kranenburg, C. "Gas release during transient cavitation in pipes." *Journal of the Hydraulics Division,* **100**(10), (1974), pp. 1383–1398. doi: 10.1061/JYCEAJ.0004077.
3. Vliegenthart, A. C. "The Schumann filtering operator and numerical computation of shock waves." *Journal of Engineering Mathematics,* **4**(4), (1970), pp. 341–348. doi: 10.1007/BF01534981.
4. Stewardson, B., Brunone, B., and Ferrante, M. "Using Experiment design to determine transient pressure behaviour." *Proceeding of 8th International Conference Pressure Surges Safe Design.* BHRG Group, 2000, p. 611.
5. Kranenburg, C. "effect of Free Gas on Cavitation in Pipelines." *Proceeding of 1st International Conference Pressure Surges Safe Design.* BHRG Group, 1972, pp. 41–52.
6. Estuti, A. A. *Technical Experiment Report on the Investigation of Effect of Changing Valve Setting on Pressure Head Time History of TPV.* 2004.
7. Wyle, E. B. and Streeter, V. L. *Fluid Transients.* McGraw-Hill, 1978.

Nomenclature

a	pressure wave celerity	[m/s]
a_0	pressure wave celerity of one-phase flow	[m/s]
A	pipe cross section area	[m^2]
C	gas concentration in liquid	[kg/m^3]
C_0	initial concentration	[kg/m^3]
C_2	pressure wave celerity parameter	
D	diameter	[m]
D_0	time step	[s]
D_1	time ordinate in (3)	[s]
F_c	constant defined by equation (57)	
g	acceleration due to gravity	[m/s^2]
H	absolute pressure head	[m]
m	gas or vapor mass/volume	[kg/m^3]
N_b	number of nuclei in m^3	[1/m^3]
P	absolute pressure	[N/m^2]
Q	volume flow rate	[m^3/s]
R_o	density ratio	
R_g	gas law constant	[J/(kgK)]
R_v	gas law constant	[J/(kgK)]
S	Henry's constant	[m^3/m^3]
S_n	constant in equation (52)	
t	time	[s]
T	temperature	[K]
Δt	time step	[s]
u	velocity of fluid	[m/s]
U	volume flow rate (if cavity)	[m^3/s]
V	void fraction	[m^3/m^3]
x	length	[m]
Δx	reach length	[m]
x_4	abscissa of point 3	see Fig. 1
α	inclination angle of pipe	
β	diffusivity of gas	[m^2/s]
ρ	density	[kg/m^3]
λ	fraction factor	
ε	empirical constant	
Subscripts		
at	atmospheric	
w	liquid	
v	vapor	
g	gas	
3	at point 3	
8	at point 8	